

Parametric Analysis on the Progression of Mechanical Properties on FSW of Aluminum-Copper Plates

Anil Kumar Deepati^{1*}, Waleed Alhazmi¹, Waleed Zakri¹, Essam Shaban¹, Pankaj Biswas²

¹ Department of Mechanical Engineering Technology, CAIT, Jazan University, Prince Mohamed Street, PO Box 114, Jazan, Jizan, 45142, Saudi Arabia

² Department of Mechanical Engineering, Indian Institute of Technology Guwahati, Guwahati, Assam, 781039, India

* Corresponding author's e-mail: adeepati@jazanu.edu.sa

ABSTRACT

The contemporary work manifests that friction stir welding (FSW) is a viable avenue for joining AA1100 aluminium to C12200 copper plates. In this present study, the response of distinctive welding parameters (viz. tool geometries, tool rotational speed, tool travel speed, and tool plunging depth) on weld quality has been investigated. The present work focused on both microstructural investigation and mechanical properties examination. It has been observed that the process parameters have significant effects on weld quality. The design of the experiments has been executed considering four welding input parameters in two variables and selected L-16 orthogonal array to limit the experimental replications. It has been observed that good quality of welds produced by keeping the tool pin offset around 4 mm towards the aluminium side and 2 mm towards the copper side. It has also been noticed that right-hand threaded tool pins are giving good weld quality compared to left-handed thread. The joint efficiencies for the welds E2, E14 which were welded by RHT tools were 75.3% and 74.61% and the strength (UTS) of the welds for the same tools exhibit's greater than the LHT tools i.e., 98 and 95 MPa. Moderate hardness values are observed for the same welds E1 and E14 with the parameters 1100 rpm, 98 welding speed, and 1.6 mm tool plunge depth. It also noticed that the weld quality can be significantly enhanced by using proper tool plunge and tool pin geometries compared to the other process parameters.

Keywords: tool geometry, process parameters, micro-hardness, tensile strength, weld microstructures, Cu-alloy, Al-alloy.

INTRODUCTION

Friction-stir-welding (FSW) [1] is a nonfusion welding technique where there is no melting occurs in the base metal and thereby considered as a solid-state welding technique. A friction stir weld is made by descending a rigid, non-depleted, momentarily rotating tool into the two mating metal pieces. The high interaction of the rotating tool with the workpieces results in heat by the friction and softens the metals to be joined. The tool rotations, travel and the pressure on the weld plates welding occurs, Figure 1. The important characteristic of the FSW process is its ability to weld the unweldable alloys within the solid-state phase [2, 3]. The rigid FSW tool encompasses the probe and shoulder. A major

part of the required heat input in this technique will be attained by the tool-shoulder face along with pin helps to mix the material. Biswas et al. [4] studied the FSW of aluminum alloy by varying the tool geometries and reported that the tapered pin tools and straight cylindrical pin tools produce superior mechanical properties.

More studies on tool geometries have been reported recently [5–12]. The latest studies were performed on the corrosion resistance, microstructural characterization of stainless steels, aluminium alloys [13]. FSW of similar aluminum materials has been successfully implemented in industries. But FSW of dissimilar alloys and elevated-melting point temperature alloys are still being hurdles to this process, few contributions were focused on these areas.

Moreira et al. [14] reported some mechanical results on dissimilar alloy combinations AA6061-T6 with AA6082-T6. They worked on microstructure assessment, investigated flexural strength, microhardness, tensile tests of all joints, and found that tensile results of the dissimilar joints exhibited moderate properties. They stated that the lowest microhardness results were achieved in the aluminum plate side due to the rupture at weld joint between tool and workpiece, similar data observed for other mechanical properties. They also examined morphology and material flow for both similar and dissimilar alloys for various welding parameters combinations. Few more studies were conducted on mechanical properties, material flow and mixing phenomenon, and microstructure investigation for dissimilar welds [15–16]. Studies on material flow paths are studied by a few researchers using some techniques like inserting some copper powders, copper films, steel balls in the joining surfaces of the two weld plates [17–21]. Few more research studies focused on investigating tribological properties of friction stir processed aluminium alloy and hybrid surface composites [22].

In dissimilar FSW, the weak metal plate reveals the joint strength, tensile samples break at the weak metal plate [23]. Chen and Lin studied dissimilar FSW of an aluminum alloy and low carbon steel and could produce sound welds with the rotational speed of 550 rpm and lower travel speeds i.e. 0.9 mm/sec. They observed the good impact strengths which are equal to the 90% of the aluminum alloy taken [24]. Dissimilar alloys welding i.e., for Cu-Al is been reported by a few authors [25–27], few authors reported the welding of Cu-Al combination is very difficult. The wide variation in the physical, thermal and metallurgical properties between Al-Cu has been the concern in welding this combination of alloys. Because of these variations, no conventional welding methods support joining aluminium to copper. Another reason for the difficulty in welding this type of combination is the formation of intermetallic component phases [28, 29] which are very hard substances. As the FSW process is performed under the recrystallization temperature it is a well-suited process to join the dissimilar Al-Cu alloys.

Many efforts have been reported in FSW of similar metals and dissimilar aluminum alloys. But there is much required to advance this process in dissimilar alloys i.e., Al-Cu, Al-Mg, Al-Fe. The applications of this type of dissimilar metals joints were reported by S. Kahl and W. Osikowicz [30]. The present study focused on parametric

analysis on the evolution and enhancement of mechanical and microstructural properties in FSW of AA1100- C12200 copper plates.

MATERIALS AND EXPERIMENTAL PROCEDURE

Commercial aluminum alloy i.e. AA1100 and pure rolled copper plates C12200 of length 200 mm, width 100 mm, and 6 mm thick of sizes were butt-welded by FSW. The hard copper plate was placed on the retreating side and the aluminum plate is in advancing plate. Two types of tools were used in this work. i.e. right helical thread tool (RHT) and left helical thread tool (LHT) and the surface of the tool shoulder made as flat with a threaded straight cylindrical pin. The shoulder diameter was kept 30 mm with a probe diameter of 6 mm, probe height kept as 5.5 mm-pin height, and 1.2 mm tool probe thread pitch. The larger tool-shoulder size was selected to obtain high heat input between the tool-workpiece interface. Figure 1 illustrates the experimental setup and Figure 2 shows the tool used in the present work. Tools are fabricated using D3 Tool steel.

An upright column milling machine having a 7.50 HP motor was adapted for FSW experiments. Before starting the welding process, the weld sample plates were ground. WD40 liquid was sprayed and cleaned with a clean cotton cloth to get rid of the unwanted dirt and oxide layers. The copper plate was rigidly fixed on the retreating side and aluminum on the advancing side. Tool pin was kept in offset positions i.e. 2 mm in copper plate and 4 mm in an aluminum plate. The workpieces were tightly fixed on a supporting plate on the machine bed to prevent joint surface inconsistencies or lumpiness.

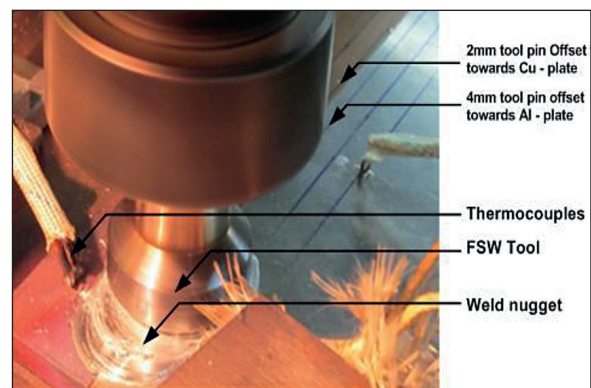


Figure 1. FSW experimental setup represents tool pin offset

Mechanical properties of the materials AA1100 and C12200 are shown in Table 1. And Table 2 and Table 3 represent the chemical composition of aluminium AA1100 and copper C12200.

Various double-blind welding trial operations were conducted with the same tools of distinct profiles (round, square, pentagonal, and hexagonal) which were used in the previous work [3]. It was noticed that unthreaded tools generate continuous voids and sometimes the thermal cracks in the weldments of this combination (i.e. Al-alloy and Cu-alloy). Therefore the threaded tools shown in Figure 2 were used in this work for carrying out the FSW experiments. Design of experiments was performed based on the following three important steps, (i) Identification of important process parameters and variables (ii) Fixing the upper and lower limits of parameters and variables (iii) and Developing the design matrix.

Development of the design matrix was performed using the Minitab software and the selected design matrix is L-16 obtained by 2⁴ (Two levels and four parameters). Table 4 shows the design of experiments followed in the present work.



Figure 2. Fabricated tools

Table 1. Mechanical properties of AA1100 and C12200

Material	Yield strength (MPa)	Ultimate tensile strength (MPa)	Elongation (%)
Alluminium base material (AA1100)	138	155	8
Copper base material (C12200)	190	245	13.5

Table 2. Chemical composition of aluminium AA1100 alloy by percentage

Material	Al	Si	Cu	Cr	Fe	Mn & others
Alluminium base material (AA1100)	99.13	0.4043	0.011	0.0013	0.40	0.008

Table 3. Chemical composition of Copper C12200

Material	Cu	P
Copper base material (C12200)	99.9–99.985	0.015–0.040

Table 4. Design of experiments

Expt. no	RPM	WS	Tool	PD
E1	1100	98	RHT	0.8
E2	1100	98	RHT	1.6
E3	1100	98	LHT	0.8
E4	1100	98	LHT	1.6
E5	1100	132	RHT	0.8
E6	1100	132	RHT	1.6
E7	1100	132	LHT	0.8
E8	1100	132	LHT	1.6
E9	1500	98	RHT	0.8
E10	1500	98	RHT	1.6
E11	1500	98	LHT	0.8
E12	1500	98	LHT	1.6
E13	1500	132	RHT	0.8
E14	1500	132	RHT	1.6
E15	1500	132	LHT	0.8
E16	1500	132	LHT	1.6

After completing the FSW experimentations the following tests were conducted i.e. Vickers microhardness (according to the ASTM E384 standard) test to observe the parameters effect on the joint hardness, tensile strength test (according to the ASTM E8 standard) to observe the welding parameter's influence on the tensile properties and microstructural evaluation (based on ASTM E407 standard) to find the surface properties.

RESULTS AND DISCUSSIONS

Mechanical properties study

This section presents the mechanical results of dissimilar Cu-Al joints i.e. hardness, tensile strengths of the welded joints for all the E16 experiments. These mechanical results are further validated by comparing them with the macro and microstructural studies.

Hardness

The overall strength of the joints is associated with hardness variations within the weld nugget. A constant load of 500 gf was applied for 10 seconds by using a digital microhardness tester (Make: Buehler VH1202). The hardness test measurements were taken on scale HV100 according to the ASTM E384 standard. The measurements are taken on every 1 mm distance away to the weld center line on both sides of the weld. Vickers microhardness test was conducted on cross-sections of FSW joints samples taken from ortho edge to the welding direction.

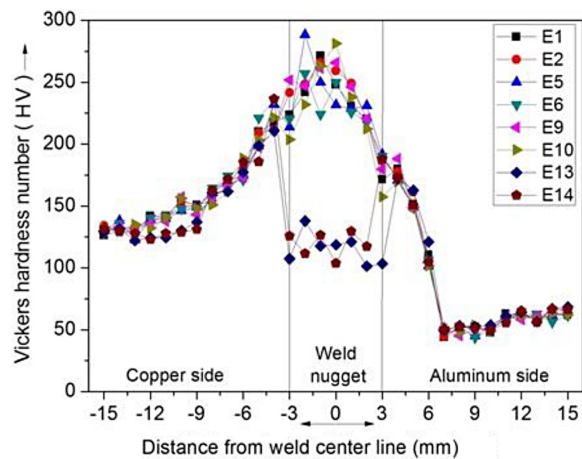


Figure 3. Hardness values for the samples welded by right helix threaded tool

A Microhardness test was conducted on the samples taken out from two groups of welds. The first group of samples from the welded joints made out of the RHT tool and the second group of samples welded with LHT tools. Hardness variations on horizontally from the weld centreline are shown in Figure 3 and Figure 4.

It was recognized that the homogeneous trend appeared in the hardness plots for almost all the samples, but for the welds of samples E13, E14 manifests the dropdown in nature. This lowered hardness reveals the truth of void existence. Figure 3 demonstrates the hardness plots for the welds using the RHT tool. Figure 4 illustrates the hardness plots of the weldments produced using the LHT tool. During tool stirring and traversing, the softened Al-alloy reciprocated severely with copper fragments randomly distributed at a few portions in the nugget zone, which results in a rise in the hardness of the Cu-Al welds for the samples E6, E5, E9, E2, and E1.

It was noticed that a greater improvement in the hardness at the nugget region was achieved for dissimilar Cu-Al FSW joints. From Figure 4 it was observed that the samples E3, E4, E7, E8, and E15 manifest the lesser hardness at the nugget zone. This may occur due to improper mixing of both the materials, minute voids have formed at the nugget region. It's also seen that the metal mixing is not appropriate using the LHT tool (Table 5; macrograph for sample E3, E4, E7, E8, E15) because the threads on the tool pin are left-hand threads and the tool rotation is made clockwise. The possible reason for the increment of hardness in the weld nugget region is the proper material mixing happened in the weld nugget and

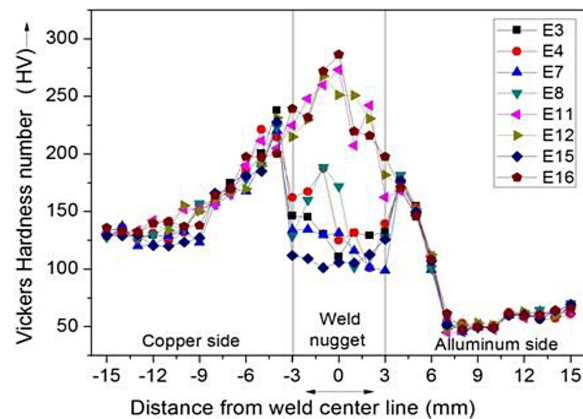


Figure 4. Hardness values for the samples welded by left helix

for the sudden rise in the hardness is due to the formation of copper fragments or shards in the nugget zone. Similar observations on drastically variations on hardness at weld nugget were reported before [31].

Tensile strength

Universal testing machine UTM (make: Instron-8801) was used for conducting tensile tests shown in Figure 10. The test sample specimens were cut from the welds at right-angles along with the welding. The ASTM-E8 standard was used in the preparation of tensile test specimens.

The tensile tests were conducted at a stable crosshead displacement rate of 10 mm/min using. Tensile test samples are shown in Figure 5 and the stress vs. elongation plot for the base material is displayed in Figure 6. Process parameters effect for the two tool pin profiles on FSW of Cu-Al joints are shown in Figure 7 and Figure 8. The trend was

common in all the joints, irrespective of the probe profile. The joint produced by the Right helix threaded (RHT) probe puts on an elevated tensile strength correlated to the other joints. A similar was also observed in the hardness results. Stress vs. strain for the base materials is shown in Figure 6.

A huge difference in the tensile strength of base materials can be observed in Figure 6. The strengths of weldments diversify from 60 to 100 MPa subject to the welding environs. Tensile test sample fractured away to the nugget and percent of elongation measured reflects ductility ranging from 0.7% to 3.0%. The deviation of ultimate tensile values and percent of elongation for all the experiments was put together in a plot shown in Figure 7 and Figure 8 respectively for all the welded joints. Tensile tests were conducted to evaluate the stress vs. strain features for the specimens welded under the weld process parameters shown in Table 4. As seen in the hardness results the joints E3, E4, E7, E8 don't



Figure 5. Tensile test specimen ASTM E-8 standards

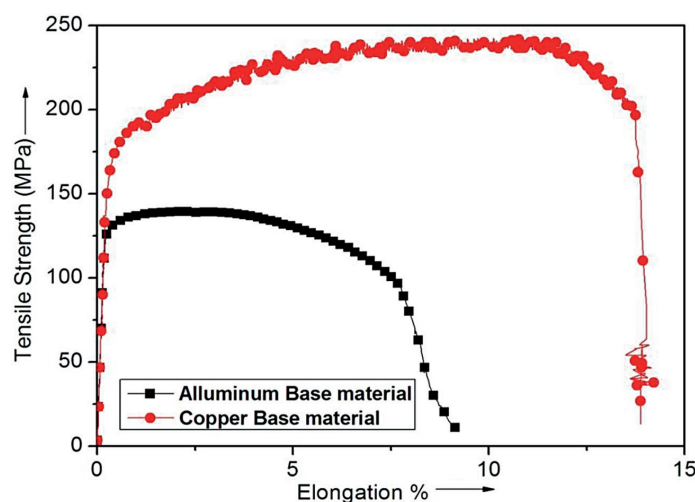


Figure 6. Stress vs. elongation plots for the base materials

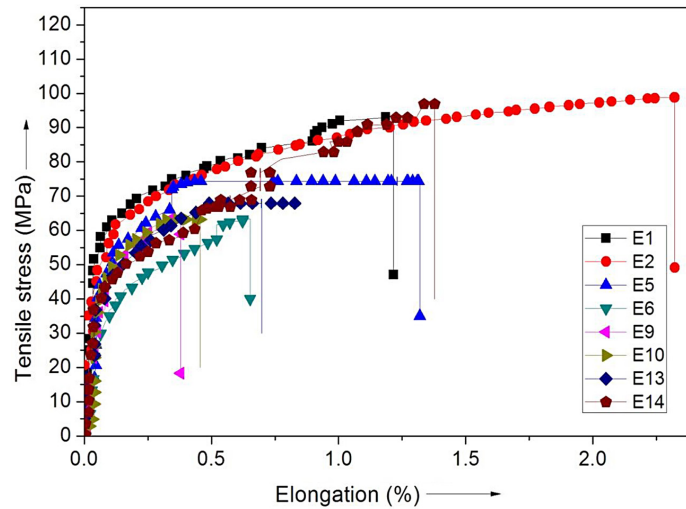


Figure 7. Stress vs. elongation plots for the specimens welded by RHT

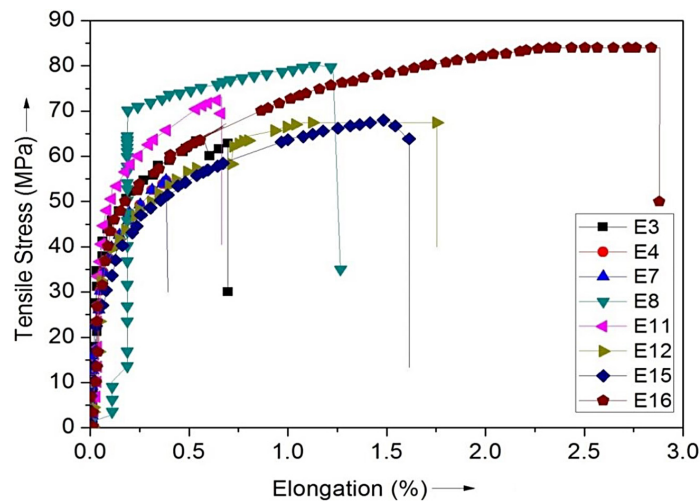


Figure 8. Stress vs. elongation plots for the specimens welded by LHT

give impressive results owing to inaccurate mixing of the two alloys but the joints E1, E9, E2, E5, E6, E10, E12, E13, E11, E14 reveals good tensile properties.

The tensile failure was seen away to the welding nugget zone i.e. at the juncture of heat HAZ and base material at Al-alloy side, signifying that the nugget region has greater joint strength. This was proved by the hardness results; the average hardness at the nugget was improved and was recorded three times of the base material (i.e. Al-alloy).

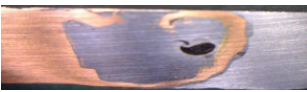




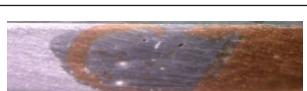

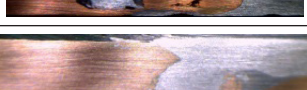
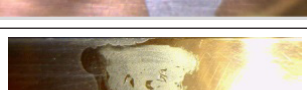
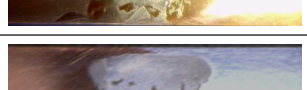






The comprehensive results of all the microhardness, tensile properties, and joint efficiency of the sixteen weldments E1-E16 are presented in Table 5. The efficiency of the weld joint was calculated UTS of the joint to the UTS of the weak base material and remark on the weld quality was also stated in Table 5. The joint efficiencies for the welds produced by the RHT are superior to

that of the welds of the LHT tool. It was noticed that the elongation of welded joints is not remarkable in these dissimilar material combinations because of the huge variation in the physical and metallurgical properties. Similar observations are reported in the former literature [31].

Microstructural study

The microstructural study gives a distinct analysis of both processed and base materials to understand the quality of the FSW joints. The study was performed using the upright metallography microscope (Make: ZEISS-maxiolab5) according to the ASTM E407. For achieving metallographic microstructure a rigid sequential procedure was followed i.e., sample cutting, mounting, grinding (coarse, fine, and polishing) etching, and microscopic examination. For

Table 5. Results of mechanical and weld zone in thickness direction

Exp no	HV*	UTS	% Elongation	Joint efficiency	Weld zone	Remarks
E1	274	92.5	1.6	71.15		Wormhole due to slower tool traverse
E2	273	98	2.3	75.3		Sound weld, failed away to weld zone
E3	140	63.5	0.7	48.84		Improper mixing
E4	185	55	0.4	42.3		Narrow keyway just below the tool shoulder
E5	285	74.5	1.25	57.69		Sound weld, failed away to weld zone
E6	260	62.5	0.62	48.07		Sound weld, failed away to weld zone
E7	130	56	0.42	42.3		Faster TRS leads Intermetallic components
E8	185	80	1.25	61.53		No defects observed
E9	272	61	0.35	44.61		Sound weld, failed away to weld zone
E10	280	63	0.36	48.46		Sound weld, failed away to weld zone
E11	274	73	0.65	56.15		Sound weld, failed away to weld zone
E12	270	68	1.75	51.92		Sound weld, failed away to weld zone
E13	140	68	0.7	52.3		Wormhole, failed at weld zone
E14	130	95	1.38	74.61		Wormhole failed at weld zone
E15	127	68.5	1.6	52.69		Defective weld, Improper mixing & lesser plunging force
E16	280	84.2	2.8	64.7		Sound weld, failed away to weld zone

* HV average of three hardness values at the nugget zone.

conducting the microstructural study the specimens are taken at the nugget zone, and these are ground with the wet grit papers on double disc grinding machines. Course and fine grinding were done using various grit papers (P400 to P2000) and subsequently cloth polishing with silver(silvo) polish and braso combination. Modified Keller's reagent i.e. 50 ml Poulant's reagent + 25 ml HNO_3 + 40 ml solution of 3 g chromic acid per 10 ml of water was used as an etchant for alluminium area. A solution of 50 ml HNO_3 + 0.5 g AgNO_3 + 50 ml H_2O was used as an etchant for copper alloy by swabbing for about 1–4 minutes. And at the nugget portion,

both the etchants were applied simultaneously and checked. Figure 9 reveals the different zones of the Cu- Al dissimilar joint.

The base material zone is an area beside the weld zone that doesn't undergo any physical or metallurgical deformation, this can also be called an unaffected zone. Figure 10a shows the unaffected base Aluminum material and Figure 10b shows the unaffected copper base material. The HAZ (Heat affected zone) is the region that undergoes thermal effect but it will not pass through any plastic deformation. The TMAZ (Thermo Mechanically Affected Zone) is the region in which the grain elongation occurs

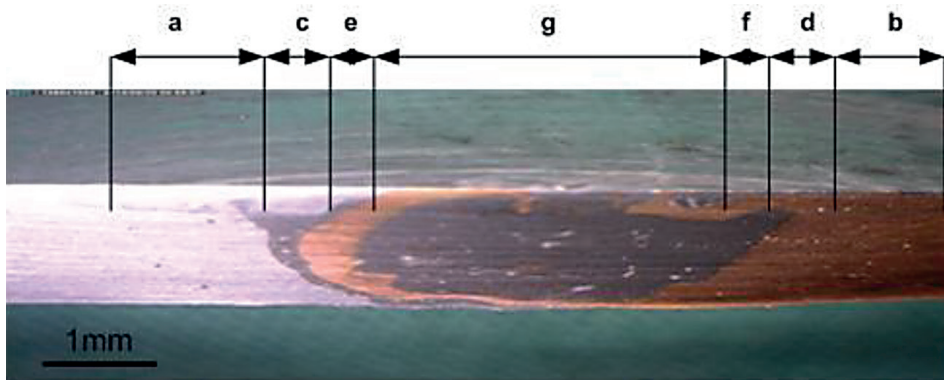


Figure 9. Macrograph of Cu-Al FSW Joint shows various zones: a) base material zone at Al side; b) base material zone at copper; c) HAZ towards Al; d) HAZ at Copper; e) TMAZ at Al side; f) TMAZ at copper side; g) Nugget zone

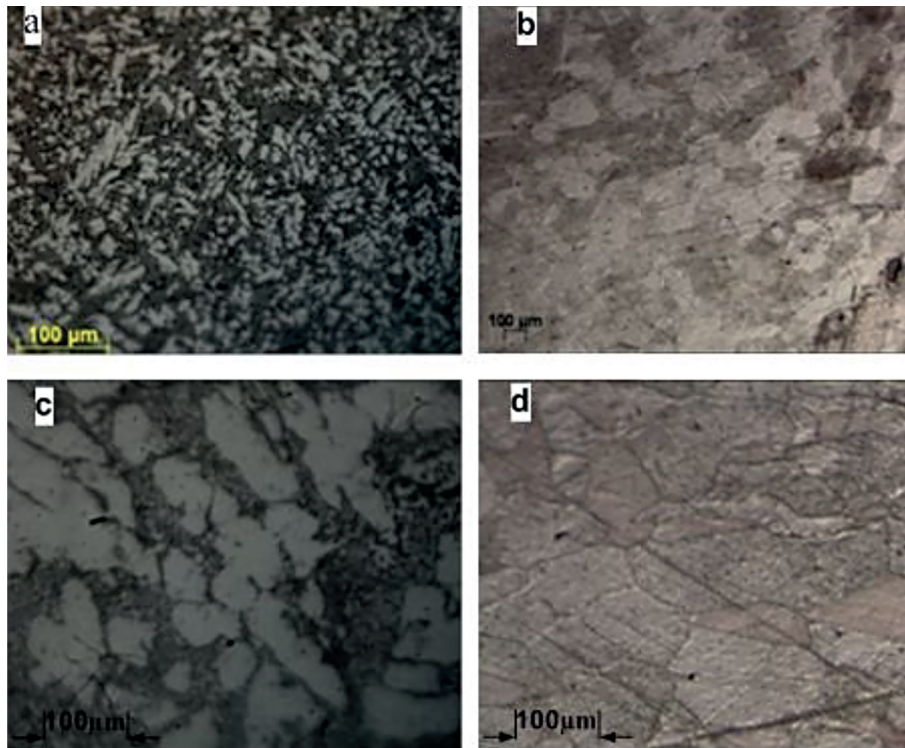


Figure 10. a) base material of alluminium; b) base material of copper; c) TMAZ at Al side and d) TMAZ at copper side

owing to the consequence of thermal and mechanical force on the weld zone. Figure 10c and Figure 10d reveal the TMAZ at Al and Cu sides. Figure 11 represents the nugget zone of the Cu-Al weld. Hard copper metal shards have formed and moved in a few welded joints at the nugget zone. Similar observations are also reported in prior scientific publications [32, 33].

Figure 12 reveals that the tough copper re-inforced and accumulated towards the aluminum side of the Cu-Al joint. Figure 13a reveals the joint produced by the process conditions E12 in which both the materials were perfectly mixed. Figure 13b shows the wormhole defect which was caused due to the slower tool traversing speed and the lesser tool plunging force. Figure 13c reveals the void which was occurred due to the improper mixing and lesser tool plunging force.

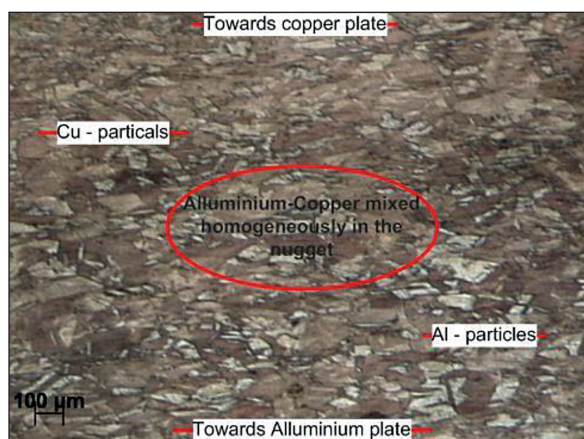


Figure 11. Copper and aluminum grain refinement at Nugget zone

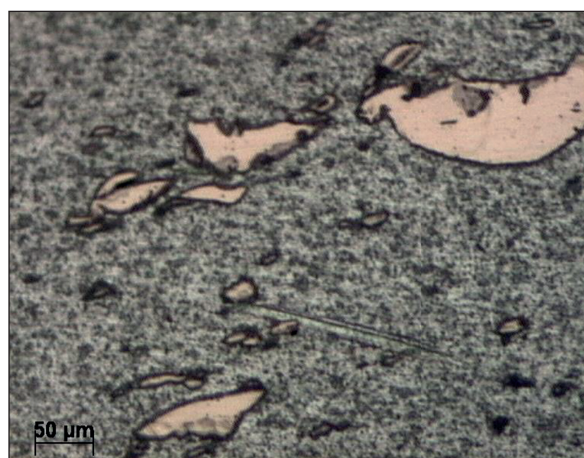


Figure 12. Tough copper shreds hauled towards the aluminum side at nugget

Intermixing behavior of aluminum and copper metal can be observed in Figure 13a. Figure 13b though there is a wormhole noticed in this macrograph, it is not continued thorough out the joint. This was supported by the tensile result of the E1 experiment. The tensile strength of the E1 sample is about 92.15 MPa. Figure 13c reveals the void which was occurred due to the improper mixing and lesser tool plunging force. The reason for the poor hardness in some samples at the nugget zone can be perceived. These voids are occurred due to the slower tool traversing speeds or with the less tool plunge depths. The microstructural studies interpret the joint quality and also comprehend the influence of grain refinement in the improvement of mechanical properties.

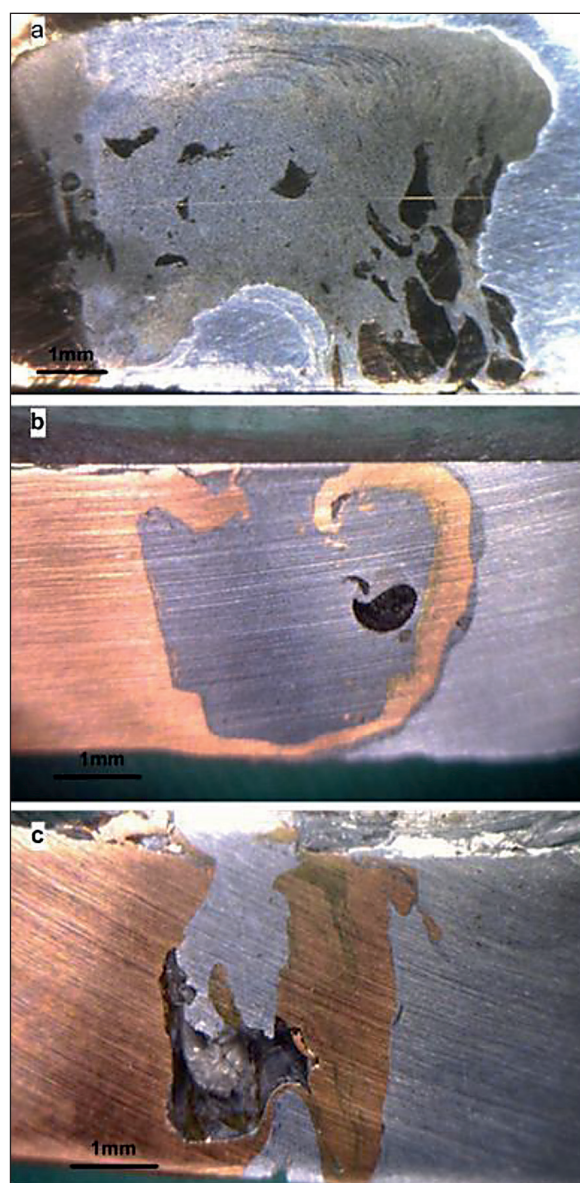


Figure 13. a) Good weld; b) Tunnel defect; (c) Void

CONCLUSIONS

In contrast to the above findings the following conclusions can be made. It was seen that the plunge depth is the most influencing parameter in the weld quality of this type of combination of metals. With the increase of plunge depth both joint strength and hardness increase. Sound joints without any defects can be produced by keeping the copper material in the retreating side instead and with a moderate tool, pin offset of 2 mm to the copper and 4 mm in the aluminum. Copper at advancing side leads to improper material mixing i.e. in that case aluminum material will flow to the copper but copper doesn't. And larger tool pin offset and lesser plunge depths lead to the defects like voids and tunnel holes. From the above experimental work, it was noticed that using FSW Tools with the Right helix threaded tools are producing good quality welds than with Left helix thread tools for the welding of dissimilar Cu-Aluminum alloys. In contrast to the hardness and tensile test results, it was perceived that RHT tools are performing superior to that LHT tools which can be observed from the UTS values for the samples E1, E2, and E16 are 92.5, 98, and 95 MPa respectively. The maximum microhardness 285HV for the experiment E5 found at weld nugget produced with RHT tool. Other significant hardness values for the welds observed for experiments E1 and E10 are 274HV and 280HV. The possible reason for the higher hardness at weld nugget is decent material mixing happened with RHT tools. Unique improvement in the hardness at the nugget zone was observed due to the formation of fine and hard copper fragment phases. During tool stirring and traversing, the softened Al alloy reacted strongly with copper shards spread throughout the nugget zone, which resulted in the higher hardness in the weld nugget.

Acknowledgments

The authors extend their appreciation to the deputyship for research and Innovation, Ministry of Education in Saudi Arabia for funding this research work through project number RUP-4.

REFERENCES

1. Thomas W.M., et al. Friction stir Butt welding. International Patent Application No. PCT/gb92102203 and Great Britain Patent Application No. 9125978.8.
2. Tang W., Guo X., McClue J.C., Murr L.E., Schmidt C. Heat input and temperature distribution of friction stir welds. *Journal of materials processing and manufacturing science*. 1999; 7(2): 162–172.
3. Biswas P., Kumar DA., Mandal NR. Friction stir welding of aluminium alloy with varying tool geometry and process parameters. *Proceedings. IMechE, Part B: J. Engineering Manufacture*. 2011; 226: 641–648.
4. Bhadeshia H.K.D.H., DebRoy T. Critical assessment: friction stir welding of steels. *Science and Technology of Welding and Joining*. 2009; 14(3): 193–196.
5. DebRoy T., Bhadeshia H.K.D.H. Friction stir welding of dissimilar alloys - a perspective. *Science and Technology of Welding and Joining*. 2010; 15: 266–270.
6. Nandan R., Lienert TJ., DebRoy T. Toward reliable calculations of heat and plastic flow during friction stir welding of Ti-6Al-4V alloy. *International Journal of Materials Research*. 2008; 99: 434–444.
7. Mohanty H.K., Mahapatra M.M., Kumar P., Biswas P., Mandal N.R. Study on the effect of tool profiles on temperature distribution and material flow characteristics in friction stir welding. *Proc. IMechE Part B: J. Engineering Manufacture*. 2012; 226(9): 1527–1535.
8. Mohanty H.K., Mahapatra M.M., Biswas P., Mandal N.R. Modeling the effects of tool shoulder and probe profile geometries on friction stirred aluminium welds using Response Surface Methodology. *Journal of Marine Science and Application*. 2012; 11(4): 493–503.
9. Biswas P., Mandal N.R. Effect of Tool Geometries on Thermal History of FSW of AA1100. *Welding Journal*. 2011; 90: 129–135.
10. Mohanty H.K., Mahapatra M.M., Biswas P., Mandal N.R. Predicting the effects of tool geometries on friction stirred aluminum welds using artificial neural networks and fuzzy logic techniques. *International Journal of Manufacturing Research*. 2013; 8(3): 296–312.
11. Moreira P.M.G.P., Santos T., Tavares S.M.O., Richter-Trummer V., Vilaca P., de Castro PMST. Mechanical and metallurgical characterization of friction stir welding joints of AA6061-T6 with AA6082-T6. *Materials and Design*. 2009; 30: 180–187.
12. Janeczek A., Tomków J., Fydrych D. The Influence of Tool Shape and Process Parameters on the Mechanical Properties of AW-3004 Aluminium Alloy Friction Stir Welded Joints. *Materials*. 2021; 14(12): 3244.
13. Mohan D.G., Gopi S., Tomków J., Memon S. Assessment of Corrosive Behaviour and Microstructure Characterization of Hybrid Friction Stir Welded Martensitic Stainless Steel. *Advances in Materials Science*. 2021; 21(4): 67–78.

14. Ouyang JH., Kovacevic R. Material flow and microstructure in the friction stir butt welds of same and dissimilar aluminum alloys. *Journal of Materials Engineering and Performance*. 2001; 11(1): 51–63.
15. Vahid F., Sindo K. Al-to-Cu friction stir lap welding. *Metallurgical and Materials Transactions*. 2011; 43(1): 303-315.
16. Colligan K. Material Flow Behavior during Friction Stir Welding of Aluminum. *Welding Research Supplementary*. 1999; 229–237.
17. Seidel T.U., Reynolds A.P. Visualization of the Material Flow in AA2195 Friction-Stir Welds Using a Marker Insert Technique. *Metallurgy and Materials Science and Transactions A*. 2001; 32: 2879–2884.
18. Guerra M., Schmidt C., McClure J.C., Murr L.E., Nunes A.C.Jr. Flow Pat-terns during Friction Stir Welding. *Materials Characterization*. 2003; 49: 95–101.
19. London B., Mahoney M., Bingel W., Calabrese M., Bossi RH., Waldron D. Material Flow in Friction Stir Monitored with Al-SiC and Al-W Composite Markers. *Proceedings Symposium on FSW and Processing II*, K.W. Jata, M.W. Ma-honey, R.S. Mishra, S.L. Semiatin, and T.Lienert, Ed., TMS, 2003; 3–12.
20. Sasikumar A., Gopi S., Dhanesh GM. Effect of welding speed on mechanical properties and corrosion resistance rates of filler induced friction stir welded AA6082 and AA5052 joints. *Materials Research Express*. 2021; 8: 066531
21. Balamurugan M., Gopi S., Dhanesh GM., Influence of tool pin profiles on the filler added friction stir spot welded dissimilar aluminium alloy joints. *Materials Research Express*. 2021; 8: 096531.
22. Anandha Kumar CJ., Gopi S., Shashi K.S., Dhanesh G.M. Mechanical, metallurgical and tribological properties of friction stir processed aluminium alloy 6061 Hybrid surface composites. *Metrology and Properties*. 2021; 9: 045019
23. Amancio S., Sheikhi S., Dos Santos J., Bolfarini C. Preliminary study on the microstructure and mechanical properties of dissimilar friction stir welds in aircraft aluminium alloys 2024-T351 and 6056-T4. *Journal of Materials Processing Technology*. 2008; 206(1–3): 132–142.
24. Thaiping C., Lin Wei-Bang. A prime study on FSW joint of dissimilar metals. *Proceedings of the XI International Congress and Exposition, Orlando, Florida, USA*. 2008.
25. Bisadi H., Tavakoli A., Tour Sangsaraki M., Tour Sangsaraki K. The influences of rotational and welding speeds on microstructures and mechanical properties of friction stir welded Al5083 and commercially pure copper sheets lap joints. *Materials and Design*. 2013; 43: 80–88.
26. Beygi R., Kazeminezhad M., Kokabi A.H. Butt joining of Al–Cu bilayer sheet through friction stir welding. *Transactions of Nonferrous Materials Society, China*. 2012; (22): 2925–2929.
27. Galvao I., Leal RM., Rodrigues DM., Loureiro A. Influence of tool shoulder geometry on properties of friction stir welds in thin copper sheets. *Journal of Materials Processing Technology*. 2013; 213(2): 129–135.
28. Kim H.J., Lee J.Y., Paik K.W. Effects of Cu/Al Intermetallic Compound (IMC) on Copper Wire and Aluminum Pad Bondability. *Transactions on Components packaging and manufacturing Technology*. 2003; 26(2): 367–374.
29. Rajan K., Wallach E.R. A transmission electron microscopy study of intermetallic formation in aluminum-copper thin film couples. *Journal of Crystal Growth*. 1980; 49: 297–302.
30. Kahl S., Osikowicz W. Composite Aluminum-Copper Sheet Material by Friction Stir Welding and Cold Rolling. *Journal of Materials Engineering and Performance*. 2013; (22): 2176–2184.
31. Winarto W., Anis M., Eka FB. Mechanical and Microstructural Properties of Friction Stir Welded Dissimilar Aluminum Alloys and Pure Copper Joints. *MATEC Web of Conferences IIW 2018. Bali - Indonesia*. 2019; 269: 01001.
32. Chularis A.A., Rzaev R.A., Syndetov M.K. Friction stir welding of aluminium and copper alloys. *Welding International*. 2020; 34(4–6): 230–241.
33. Bora B., Kumar R., Chattopadhyaya S., Borucki, S. Analysis of Variance of Dissimilar Cu-Al Alloy Friction Stir Welded Joints with Different Offset Conditions. *Applied Sciences*. 2021; 11(10): 4604.